Magnetic transitions in single-crystal erbium

1995 J. Phys.: Condens. Matter 7 4713

(http://iopscience.iop.org/0953-8984/7/24/011)

J. Phys.: Condens. Matter 7 (1995) 4713–4723. Printed in the UK

Magnetic transitions in single-crystal erbium

Brian Watson and Naushad Ali
Department of Physics, Southern Illinois University, Carbondale, IL 62901, USA

Received 15 February 1995, in final form 29 March 1995

Abstract. Commensurate spin slip structures were observed by Gibbs *et al* in x-ray scattering studies. We have observed magnetic transitions in macroscopic measurements of magnetization, AC susceptibility, electrical resistivity, and thermal expansivity along the three crystal axes of single-crystal erbium that correspond to these spin slip structures. Our measurements show antiferromagnetic ordering of the c axis and basal plane componants at $T_{N\parallel} = 89$ K and $T_{N\perp} = 53$ K, respectively, as well as ferromagnetic ordering along the c axis below 18 K. In addition, we observe anomalies at 27, 29, 34, 40 and 51 K. These anomalies correspond well with previous studies. The order of these transitions can be determined using thermal expansion data. We observe anomalies at 21.6 K and 23.3 K that we believe correspond to basal plane reordering in the 2(44) magnetic phase. There are also anomalies above $T_{N\perp}$ suggesting a short-range ordering of the basal plane moments. We have analysed the resistivity versus temperature plot in the ferromagnetic region to determine the temperature dependence and the spin wave activation energy along the b and c axes.

1. Introduction

In zero applied magnetic field, erbium undergoes a series of transitions into long-range commensurate magnetic structure as the temperature is lowered from the Néel temperature at 89 K. In this paper, we will present our observations of these magnetic phase transitions in single-crystal erbium. Erbium is a rare earth metal that forms a hexagonal close-packed structure with two layers per chemical unit cell and a magnetic moment of $9\mu_B$ per atom. The f shell electrons are spatially localized and are responisible for the complex magnetic structure. The 4f orbitals do not interact directly but instead through the polarization of the conduction electrons or RKKY interaction. This interaction is long range and oscillatory and gives rise to the periodic spin structures observed in rare earth metals. The magnetic structure of erbium is complex and is described in several neutron and x-ray diffraction studies [2–12]. The magnetic structure of erbium was first studied by Cable *et al* [2] using neutron diffraction. In their study they identified three distinctly ordered states in erbium. Below the Néel temperature $T_{N\parallel}$ of 89 K, the c axis moment orders antiferromagnetically in a sinusoidally modulated structure with a periodicity of approximately seven atomic layers. There exists a second Néel temperature $T_{N\perp}$ at 53 K, below which the basal plane moments order with the same wave vector as the c axis. At this temperature, erbium becomes a helical structure with a specific turn angle between successive spins in the basal plane and a sinusoidal modulation along the c axis. As the temperature is lowered, the c axis wavevector and the turn angle decrease monotonically. Eventually, the c axis moment begins to lose its sinusoidal modulation and 'square up' as indicated by odd harmonics observed in several neutron diffraction studies, until 25 K, when erbium makes a transition into an alternating cone structure. Below the Curie temperature of 18 K, erbium orders ferromagnetically into

0953-8984/95/244713+11$19.50

a conical structure along the c axis. The magnetic structure of erbium has been enumerated further in a synchrotron x-ray scattering study by Gibbs *et al* [1]. In their study, erbium exhibits a sequence of lock-in transitions to rational wave vectors. At certain temperatures, the turn angle attains values that make the magnetic structure commensurate with the lattice. These commensurate structures have been described by Gibbs *et al* [1] using a spin slip model. In their model, erbium orders antiferromagnetically with the magnetic moments along the c axis in four atomic planes ordered either parallel or antiparallel to the c axis. The basal plane moments are spirally ordered with the same modulation as the c axis. In some instances, four atomic planes may be replaced with three atomic planes. This is referred to as spin slip. In table 1, we have adopted the notation of Gibbs *et al* [1] and Cowley and Jensen [8]. The wavevector 2/7 indicates the basal plane moments rotate by 2π every seven atomic planes. The notation (43) indicates that the c axis moment is ordered in four atomic planes along the c axis and in three atomic planes along the negative c axis. This particular ferrimagnetic structure would possess a relatively large net c axis moment. The 3/11 or (443) structure indicates a spin slip every 11 atomic planes; however, the whole structure is ordered antiferromagnetically. Because the hexagonal close-packed structure contains two inequivalent sublattices, this commensurate structure should be described as (443443) or 2(443), with the net c axis moment being relatively small. All of these commensurate structures can be observed in measurements of magnetization, AC susceptibility, resistivity, and thermal expansion. It can easily be seen from the graph of c axis AC susceptibility that commensurate structures with a net ferrimagnetic moment, such as 2(43) and 2(4443), appear as sharp peaks in the magnetization versus temperature plots. Those commensurate structures without a net magnetic moment, such as 2(443) and 2(44443), will appear as relatively small peaks and will be difficult to observe. Those spin slip structures with a net magnetic moment are stable and lock in to a rational wave vector. These regions are approximately 3 K wide and are separated by incommensurate regions, until 29 K, below which only commensurate regions exist.

Table 1. Commensurate spin slip structures in single crystal erbium. The wavevectors q and the corresponding spin slip structures are taken from the articles by Gibbs *et al* [1] and Cowley and Jensen [8]. Column three shows the temperatures in our magnetization and AC susceptibility data corresponding to the respective spin slip structures. Column four reports the order of these transitions as determined from our thermal expansion data. An asterisk indicates that we are unable to determine this information from our data.

q	Structure	Temperature (K)	Order of transition
5/21	ferromagnetic	$T_c = 18$	first order
1/4	2(44)	18–25	*
6/23	2(444443)	25.5–28.5	first order
5/19	2(44443)	29	*
4/15	2(4443)	32.5–35.5	*
3/11	2(443)	40	*
2/7	2(43)	49.5–52.5	first order
		$T_{N\perp} = 53$	weak first order
		$T_{N\parallel} = 89$	second order

2. Experimental details

The erbium single crystal (4.4 mm × 3.3 mm × 5.0 mm) was grown at Ames Laboratory. The magnetization measurements were performed using a SQUID Magnetometer (Quantum

Design, Inc., San Diego, CA) with an applied field of 100 G. Thermal expansion measurements were performed using the capacitance dilatometer method. The AC susceptibility measurements were carried out using the mutual inductance method in an RMS field of 1.5 G. Resistivity measurements were also performed using the temperature and magnetic field control of the SQUID, with a Keithley 220 programmable current source and Keithley 181 nanovoltmeter as external devices. Two longer b axis and c axis crystals were used for resistivity measurements only (c axis, 12.0 mm × 1.1 mm × 1.6 mm; b axis, 10.8 mm × 1.2 mm × 1.7 mm). All measurements covered a range of 10–100 K to include the Néel temperature. All measurements were taken with the temperature increasing to avoid hysteresis effects. Measurements were reproduced for all three axes, except resistivity measurements (b and c axes only), although only plots for two axes are presented here.

3. Results

The c axis AC susceptiblity as a function of temperature is shown in figure 1(a) in the temperature range of 10–100 K. We observe the Curie temperature T_C at 19.2 K and the basal plane and longitudinal Néel temperatures, $T_{N\perp}$ and $T_{N\parallel}$, at 52.5 K and 87.9 K respectively. We find spin slip transitions at 26.6, 28.5, 29.7, 35.8, 43.0 and 51.0 K. Those commensurate spin slip structures with a net magnetic moment, such as 2(43), 2(4443) and 2(444443), are stable over a temperature range of approximately 3 K and appear as sharp peaks on the AC susceptibility versus temperature plot. All transitions listed in table 1 can be observed in the c axis AC susceptibility; however, spin slip structures without a net ferromagnetic moment are difficult to observe. Figure 1(b) and (c) is the expanded regions around 29 K and 42 K, showing the 2(44443) and 2(443) spin slip structures respectively. These spin slip structures appear to be stable over a much shorter temperature range and due to their relatively small net magnetic moment, manifest themselves as small changes in the slope of the AC susceptibility plot. Table 2 lists the transition temperatures for the various measurements.

Table 2. The temperatures in kelvin where we find the anomalies in various measurements that correspond to spin slip, Curie, and Néel transitions in single-crystal erbium. T_α and T_β are the temperatures at which we find the anomalies in the 2(44) alternating cone phase that we believe correspond to a reordering of the basal plane moments. An asterisk indicates that we are unable to determine this information from our data.

Measurement	T_C	T_α	T_β	2(44)	2(444443)	2(44443)	2(4443)	2(443)	2(43)	$T_{N\perp}$	$T_{N\parallel}$
c axis χ_{AC}	19.2	22.0	23.6	26.6	28.5	29.7	35.8	43.0	51.0	52.5	87.9
a axis χ_{AC}	18.3	20.1	23.6	25.4	26.7	29.3	33.6	40.7	49.6	51.2	87.0
b axis χ_{AC}	18.0	21.4	*	25.2	26.3	28.3	33.4	40.4	49.3	51.2	87.0
c axis M	19.5	*	*	*	26.8	29.1	34.4	41.7	51.3	*	87.4
b axis M	19.5	22.1	*	*	26.9	29.3	34.7	41.8	51.9	54.1	87.5
a axis M	19.5	21.8	23.3	*	26.6	28.9	34.5	41.7	51.3	53.3	88.0
c axis $\Delta L/L$	19.3	21.8	23.2	*	25.7	28.0	*	*	49.5	52.0	85.9
a axis $\Delta L/L$	19.2	*	22.9	*	25.6	27.8	*	41.7	49.3	52.1	86.1
b axis $\Delta L/L$	19.2	21.7	23.3	*	25.6	28.3	*	*	49.5	52.0	86.3
c axis ρ	19.0	22.0	23.0	*	25.8	*	36.0	39.8	49.8	52.0	86.3
b axis ρ	19.7	*	*	*	26.7	*	*	42.1	49.2	51.6	88.6

The inset of figure 1(a) shows the c axis AC susceptibility in the temperature range from 19 K to 25 K. There are two extremely small transitions at 22.0 K and 23.6 K, which are

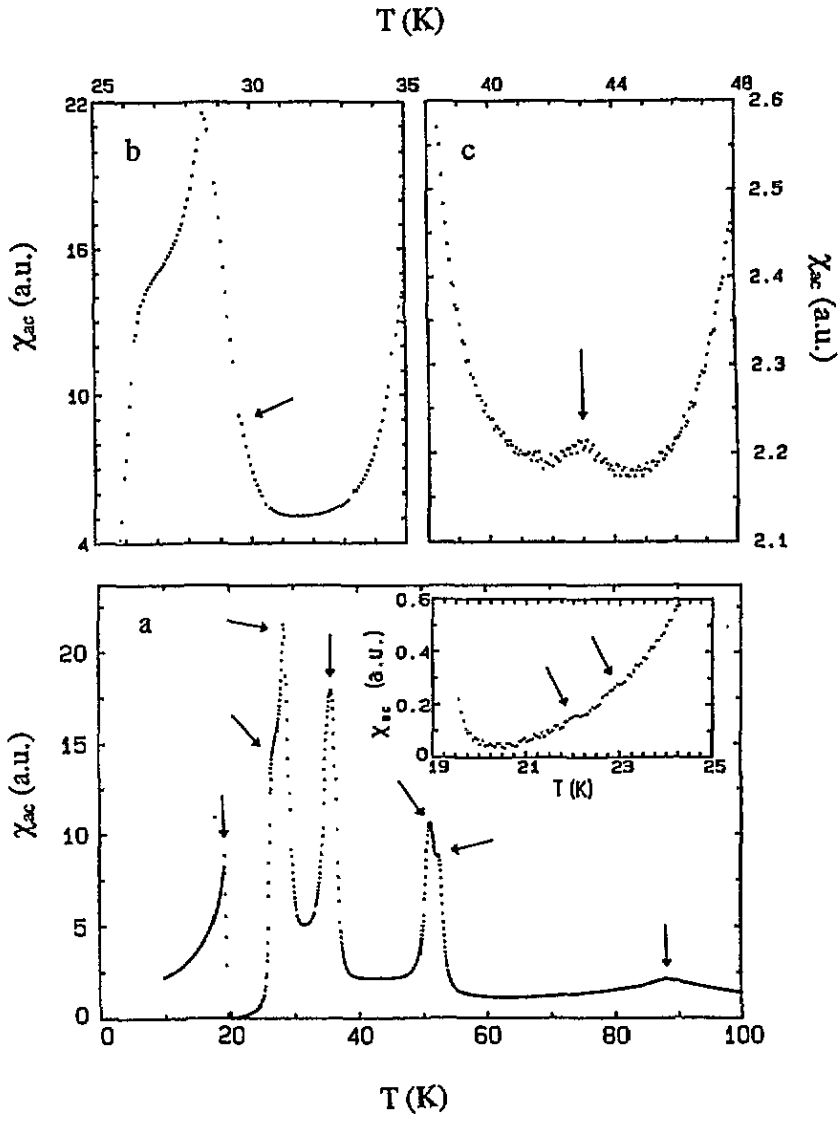

Figure 1. (a) The AC susceptibility (χ_{AC}, in arbitrary units) of single-crystal Er in the temperature range from 10 K to 100 K along the c axis. The inset shows χ_{AC} versus temperature for the c axis near 22 K. (b) χ_{AC} versus temperature along the c axis for Er near 30 K. (c) χ_{AC} versus temperature for Er along the c axis near 42 K. Anomalies are indicated by arrows.

more easily observed on the derivative plot. These anomalies can also be observed on the a axis susceptibility, b axis magnetization, and c axis thermal expansion and resistivity, although in certain measurements only the transition at 22.0 K is present. Table 2 contains the temperatures at which these two anomalies, which we refer to as T_α and T_β, are found. These anomalies have been observed previously in a microcalorimetry study by Astrom *et al* [14]. There is some question as to whether these transitions represent a commensuration with the lattice. The spin slip rational wavevectors follow the form $q = n(4n-1)^{-1}c^*$. Therefore, the next spin slip should have the wavevector $q = 7/27$ for $n = 7$. By reviewing

the wavevector data from Habenschuss *et al* [10], we can see that this spin slip should occur near 26 K. Therefore, these transitions are not the result of a spin slip commensuration. If we look at table 1, we can see that these temperatures fall within the 2(44) magnetic phase. Because neutron diffraction data have shown that the *c* axis wavevector for this temperature range is constant, we propose these transitions represent a reordering of the basal plane. Cowley and Jensen [8] discuss a possible (3030) and (44) phase existing in the alternating cone phase. However, this does not explain why there are two transitions in the 2(44) magnetic phase instead of one. We are still unsure as to the nature of these transitions.

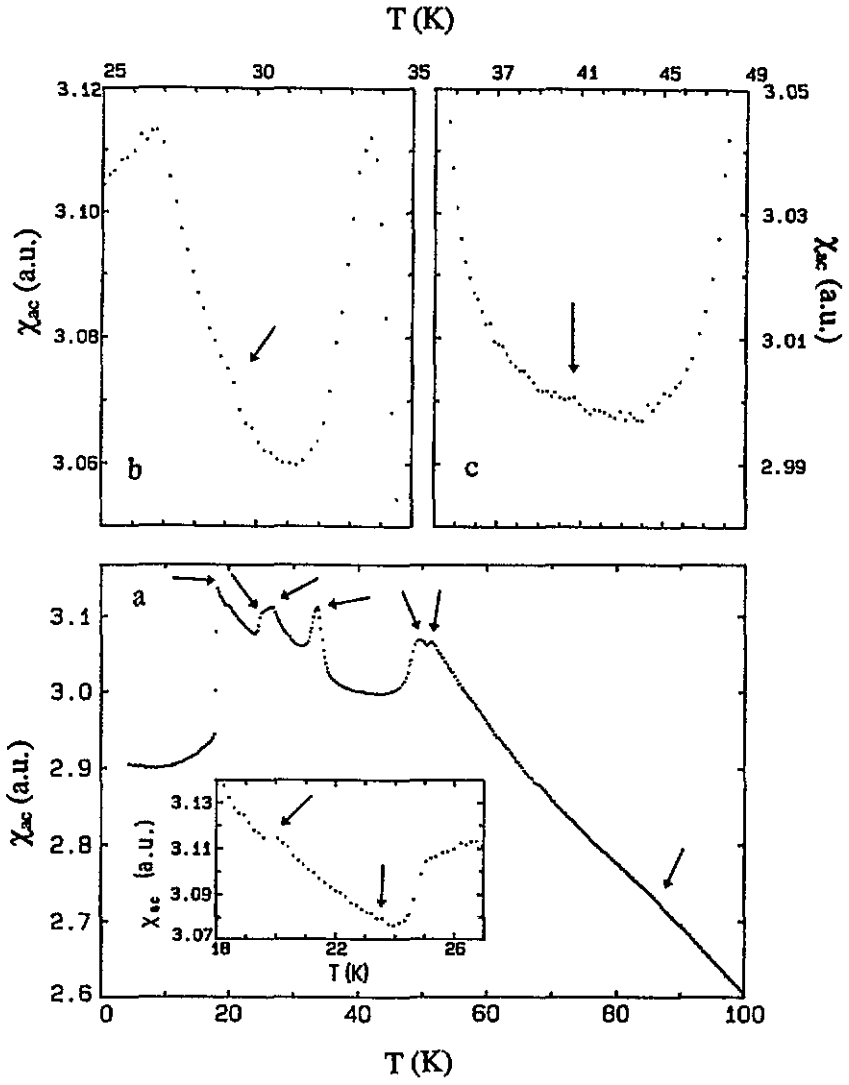

Figure 2. (a) The AC suceptibility (χ_{AC}, in arbitrary units) of single-crystal Er in the temperature range from 5 K to 100 K along the *a* axis. The inset shows χ_{AC} versus temperature for the *a* axis near 22 K. (b) χ_{AC} versus temperature for Er along the *a* axis near 30 K. (c) χ_{AC} versus temperature for Er along the *a* axis near 41 K.

The *a* axis AC susceptibility is presented in figure 2(a). The *a* axis susceptibility plot

was produced with the AC field directed along the *a* axis. All of the peaks observed in the *c* axis AC susceptibility can also be observed in the basal plane AC susceptibility. We observe the Curie temperature T_C at 18.3 K and the basal plane Néel temperature $T_{N\perp}$ at 51.2 K. The longitudinal Néel temperature $T_{N\parallel}$, although difficult to detect due to the slope of the graph at that temperature, is found at 87.0 K. We observe spin slip anomalies at 25.4, 26.7, 29.3, 33.6, 40.7 and 49.6 K. Figure 2(b) and (c) shows the previously mentioned 2(44443) and 2(443) spin slip structures, which are difficult to observe in the basal plane as well as those for the *c* axis for the same reasons as listed in the above paragraph. The transition temperatures for the *b* axis AC susceptibility are listed in table 2 for completeness although the plots are not presented in this paper due to space limitations. The inset of figure 2(a) displays transitions at 20.1 K and 23.6 K, which were discussed previously for the *c* axis AC susceptibility.

By reviewing the AC susceptibility data, we can draw some conclusions concerning the structure of the antiferromagnetic phase between T_C and $T_{N\perp}$. The basal plane spin slip transitions occur at approximately the same temperatures as those for the *c* axis. This allows us to infer that the *c* axis spin slips are responsible for the anomalies we observe in the basal plane AC susceptibility. The net ferrimagnetic moment of the *c* axis spin slips produces transitions in the basal plane AC susceptibility plot due to the average angle that the individual magnetic moments make with the basal plane. No other ordering process is occurring in the basal plane that we can observe. At least, we can say that, if another ordering process is occurring in the basal plane, it is insignificant compared to the contribution made by the *c* axis spin slips. We therefore propose that the *c* axis modulation and the basal plane modulation are locked together at zero applied field and differ only by a constant phase. This is in agreement with Cowley and Jensen [8] and Eccleston and Palmer [12]. By examining table 1, we can state that, independent of the temperature contribution, the relative peak heights for the spin slips with a net magnetic moment will be 1:(23/15):(23/7). The actual peak heights decrease with increasing temperature and do not follow these ratios due to the temperature contribution over this range. However, we can say that the ratios of the peak heights for spin slip transitions that have a net ferrimagnetic moment (2(43), 2(4443) and 2(444443)) are different for the *c* axis and basal plane AC susceptibilities. Therefore, the average angle that the individual magnetic moments make with the basal plane must be changing with temperature. This was discussed in an x-ray study by Sanyal *et al* [11].

The magnetization as a function of temperature for the *c* axis is shown in figure 3(a). The inset is the region around 42 K expanded to show the 2(443) spin slip transition. The double peaks observed on the AC susceptibility graph at 28 K and 52 K have merged into single peaks due to the 100 G *c* axis applied field we have used to conduct our magnetization measurements. It is not completely correct to compare our magnetization versus temperature results here with our results for zero-field measurements. However, we have made the assumption that the temperature at which our magnetic transitions occur in erbium will not change substantially for a 100 G applied field. Most spin slip transitions can be observed. We see spin slip transitions at 26.8, 29.1, 34.4, 41.7 and 51.3 K. The Curie temperature and longitudinal Néel temperature are observed at 19.5 K and 87.4 K respectively. The basal plane Néel temperature cannot be resolved from the 2(43) spin slip transition on our magnetization plot and so we assume it occurs at the same temperature of 51.3 K.

Figure 3(b) displays the *b* axis magnetization as a function of temperature with an applied magnetic field of 100 G along the *b* axis. Although some of the spin slip transitions are difficult to observe, most transitions can be seen by reviewing the derivative plot. We can see spin slip transitions at 26.9, 29.3, 34.7, 41.8 and 51.9 K. The Curie and Néel

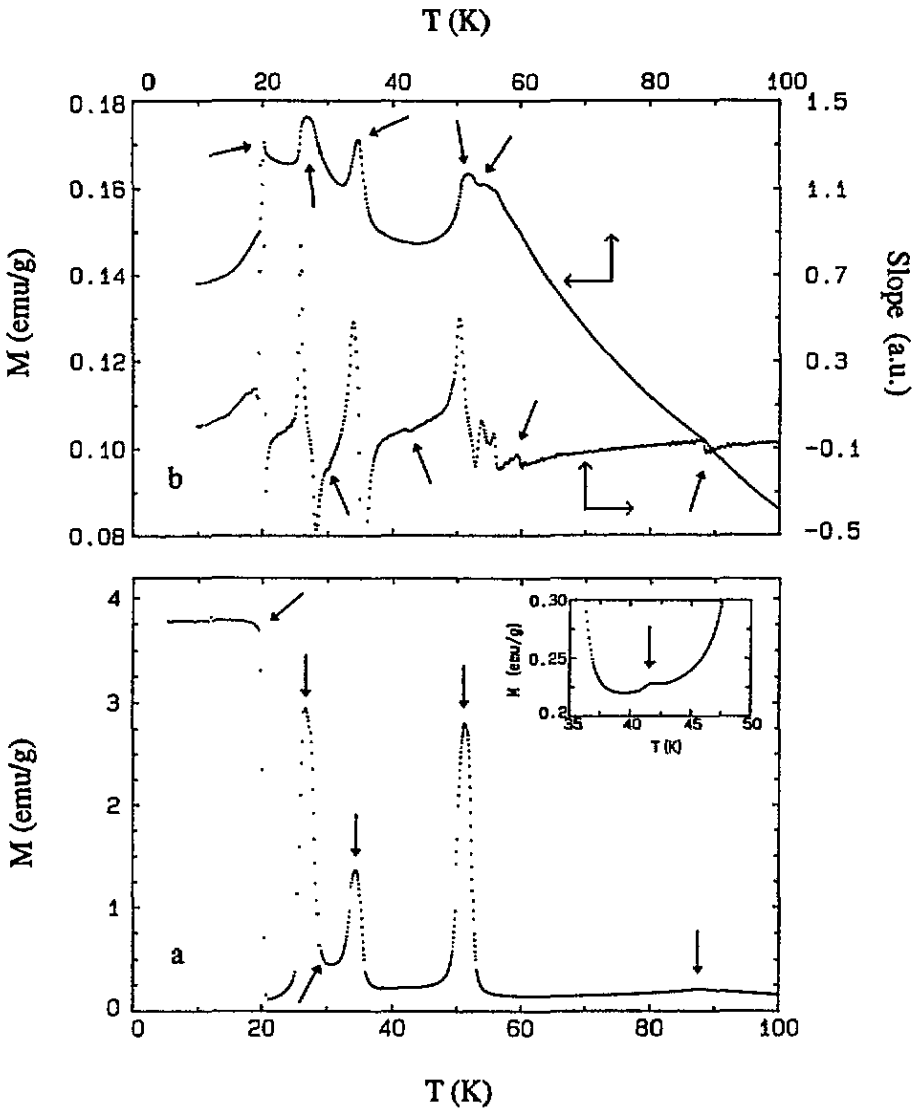

Figure 3. (a) The magnetization (M) of single-crystal Er along the c axis as a function of temperature in a constant magnetic field of 100 G. The inset shows M against T for the c axis near 42 K. (b) The upper curve is the magnetization of Er along the b axis as a function of temperature for a constant magnetic field of 100 G. The lower curve is the slope of the b axis M–T plot for Er.

temperatures occur at 19.5, 54.1 and 87.5 K. Near 53 K, the $T_{N\perp}$, there are four peaks where there should only be two. The first peak at 51.9 K is the spin slip transition 2(43) and the second peak is the basal plane Néel temperature at 54.1 K. The other two peaks are clearly identifiable from the derivative plot at temperatures of 55.5 K and 59.7 K. The peak at 55.5 K may be spurious; however, the peak at 59.7 K is reproducible and also occurs in the a axis magnetization as well as the basal plane thermal expansion plots. This may be evidence of short-range ordering of the basal plane moments as discussed by Habenschuss *et*

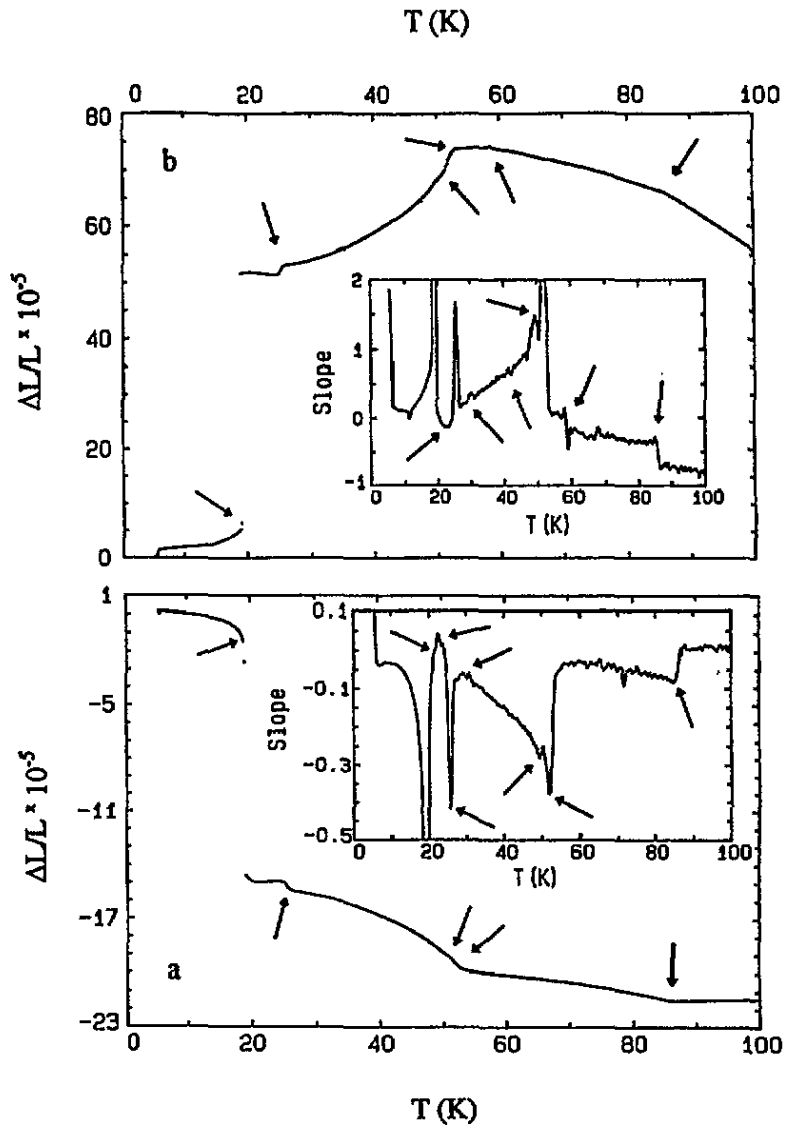

Figure 4. (a) Thermal expansivity ($\Delta L/L$) relative to the copper cell as a function of temperature along the c axis of Er in the range from 5 K to 100 K. The inset is the derivative of the c axis thermal expansivity. (b) Thermal expansivity ($\Delta L/L$) relative to the copper cell as a function of temperaure along the a axis of Er in the range from 5 K to 100 K. The inset is the derivative of the a axis thermal expansivity.

al [10] and Eccleston and Palmer [12]. The a axis transition temperatures are also provided in table 2. There is also a small transition T_α at 22.1 K, which corresponds to the reordering of the basal plane for the 2(44) alternating cone phase as discussed previously.

In figure 4(a) we present the c axis thermal expansivity ($\Delta L/L$) with respect to the copper cell as a function of temperature for the range from 5 K to 100 K. By reviewing the thermal expansion graph, we can deduce the order of the various magnetic phase transitions. The thermal expansivity derivative plot is inset in figure 4(a) to help clarify the order of

transitions. A first-order change in the thermal expansivity will appear as a sharp peak in the derivative plot. A second-order change in the thermal expansivity will appear as a step in the derivative plot. The longitudinal Néel temperature at 85.9 K is obviously a second-order transition. The Curie temperature of 19.3 K is a first-order transition. The spin slip transitions 2(444443) at 25.7 K and 2(43) at 49.5 K both appear to be first order as well. The transition at the basal plane Néel temperature of 52.0 K appears to be both a peak and a discontinuity on the derivative plot. We will label this as a weak first-order transition. These results agree with the results of Astrom and Benediktsson [13] but are contrary to the results of Habenschuss *et al* [10] and Genossar *et al* [15], who have determined that $T_{N\perp}$ is a purely second-order transition. From our data, it is impossible to determine the order of the remaining spin slip transitions. We can identify two transitions in the 2(44) magnetic phase, T_α and T_β, discussed previously, at 21.8 K and 23.2 K. The order of these transitions appears to be first order, which would agree with the microcalorimetry study by Astrom and Benediktsson [13], although the resolution of our measurement is not high enough to be certain. Curiously, the 2(4443) transition, which is a relatively large transition on our magnetization and susceptibility plots, is not apparent on our thermal expansion plots.

Figure 4(b) shows the a axis thermal expansivity ($\Delta L/L$) relative to the copper cell as a function of temperature. The thermal expansivity derivative plot is inset to figure 4(b). The order of these magnetic phase transitions agrees with the order previously mentioned for the c axis thermal expansion. We observe spin slip transitions at 25.6, 27.8, 41.7 and 49.3 K. The Curie temperature and Néel temperatures occur at 19.2, 52.1 and 86.1 K respectively. We also observe a transition at 58.6 K, above the $T_{N\perp}$, that is reproducible in the basal plane thermal expansion data and basal plane magnetization data. We are unsure of its origin, although it may represent the short-range ordering of the basal plane moments as previously mentioned for the basal plane magnetization versus temperature plot in figure 3(b). The b axis thermal expansion transition temperatures are also provided in table 2.

The c axis resistivity versus temperature graph is shown in figure 5(a). Resistivity values are given relative to the value at 90 K. The derivative is also shown on the same plot. We can identify spin slip transitions at 25.8, 36.0, 39.8 and 49.8 K. The Curie temperature is 19.0 K, while the Néel temperatures are at 52.0 K and 86.3 K. We also observe transitions T_α and T_β at 22.0 K and 23.0 K.

The b axis resistivity versus temperature graph is shown in figure 5(b). Again, resistivity values are given relative to the value at 90 K. Transitions are difficult to identify on the resistivity plot and therefore the derivative plot is also included. We observe spin slip transitions at 26.7, 42.1 and 49.2 K. The Curie temperature is 19.7 K, while the Néel temperatures are at 51.6 K and 88.6 K.

The resistivity against temperature dependence for various temperature regions is markedly different for both the b axis and c axis resistivity graphs. For a simple ferromagnet at low temperatures the resistivity will have the form $\rho = CT^2$. For an anisotropic ferromagnet below the Curie temperature, Makintosh [16] has predicted that the resistivity will have the form $\rho = T^2 e^{(-\Delta E/kT)}$, where ΔE represents the spin wave activation energy. For magnetically ordered spiral structures such as erbium and holmium, the resistivity will have the temperature dependence $\rho = T^4 e^{(-\Delta E/kT)}$ as given by Taylor [17]. We have found, however, that erbium obeys a T^2 dependence in the ferromagnetic region. We plotted resistivity versus $T^2 e^{(-\Delta E/kT)}$ below the Curie temperature, varying ΔE until we had a linear plot. Consequently, we obtained the spin wave activation energy for that particular crystal axis. For the c axis, we found a value of $\Delta E/k$ of 10.6 K and for the b axis, we found a value for $\Delta E/k$ of 14.8 K. Therefore, the resistivity for erbium in the ferromagnetic region has a T^2 dependence instead of the T^4 dependence given for a

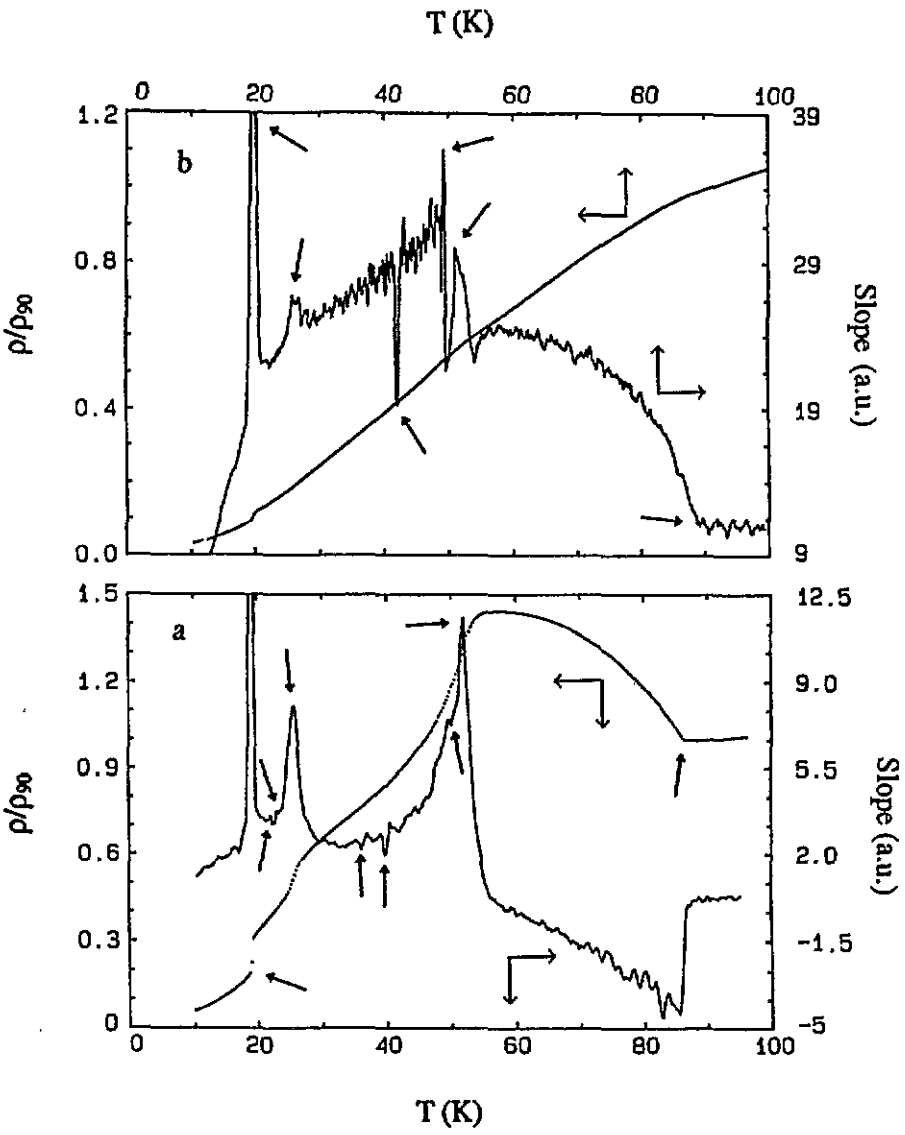

Figure 5. (a) Resistivity (ρ) relative to the resistivity at 90 K (ρ_{90}) versus temperature for the *c* axis of single-crystal Er in the temperature range from 10 K to 100 K. The derivative of the *c* axis resistivity versus temperature plot is also included. (b) Resistivity (ρ) relative to the resistivity at 90 K (ρ_{90}) versus temperature for the *b* axis of single-crystal Er in the temperature range from 10 K to 100 K. The derivative of the *b* axis resistivity versus temperature plot is also included.

magnetically ordered spiral structure. The spin wave activation energies are different for the *c* axis and basal plane directions as expected. The *c* axis resistivity plot shows a negative slope between the two Néel temperatures. The feature is attributed to the deformation of the Fermi surface and the creation of superzone gaps caused by the magnetic order in the helical antiferromagnetic phase below $T_{N\parallel}$ [18].

4. Conclusion

We can observe anomalies in AC susceptibility, magnetization, thermal expansion, and resistivity for the c axis and basal plane that correspond to spin slip structures observed in previous x-ray and neutron diffraction studies. Based on thermal expansion measurements, we have determined that the spin slip transitions at 27 K and 51 K are of first order, while the Curie temperature and the longitudinal Néel temperature are second-order phase transitions. The basal plane Néel temperature appears to be a weak first-order phase transition. In basal plane magnetization and thermal expansion, we have observed anomalies above the $T_{N\perp}$ that may indicate the short-range ordering of the basal plane moments as observed in neutron diffraction studies. We have also observed anomalies in the basal plane susceptibility and magnetization versus temperature plots at 21.6 K and 23.3 K that may correspond to a reordering of the basal plane moments in the 2(44) magnetic phase. We have determined the temperature dependence of the resistivity for erbium in the ferromagnetic phase and the spin wave activation energy for the b axis and c axis.

References

[1] Gibbs D, Bohr J, Axe J D, Moncton D E and D'Amico K L 1986 *Phys. Rev.* B **34** 8182
[2] Cable J W, Wollan E O, Koehler W C and Wilkinson M K 1965 *Phys. Rev.* B **140** 1896
[3] Atoji M 1974 *Solid State Commun.* **14** 1047
[4] Lin H, Collins M F, Holden T M and Wei W 1992 *J. Magn. Magn. Mater.* **104–107** 1511
[5] Lin H, Collins M F, Holden T M and Wei W 1992 *Phys. Rev.* B **45** 12 873
[6] Brits G H F and Du Plessis P De V 1989 *Physica* B **156–157** 762
[7] Jensen J and Cowley R A 1993 *Europhys. Lett.* **21** 705
[8] Cowley R A and Jensen J 1992 *J. Phys.: Condens. Matter* **4** 9673
[9] McMorrow D F, Jehan D A, Cowley R A, Eccleston R S and McIntyre G J 1992 *J. Phys.: Condens. Matter* **4** 8599
[10] Habenschuss M, Stassis C, Sinha S K, Deckman H W and Spedding F H 1974 *Phys. Rev.* B **10** 1020
[11] Sanyal M K, Gibbs D, Bohr J and Wulff M 1994 *Phys. Rev.* B **49** 1079
[12] Eccleston R S and Palmer S B 1992 *J. Phys.: Condens. Matter* **4** 10 037
[13] Astrom H U and Benediktsson G 1989 *J. Phys.: Condens. Matter* **1** 4381
[14] Astrom H U, Chen D-X, Benediktsson G and Rao K V 1990 *J. Phys.: Condens. Matter* **2** 3349
[15] Genossar J, Steinitz M O and Fawcett E 1984 *Can. J. Phys.* **62** 823
[16] Makintosh A R 1963 *Phys. Lett.* **4** 140
[17] Taylor K N R and Darby M I 1972 *Physics of Rare Earth Solids* (Trowbridge: Redwood) p 208
[18] Terki F, Gandit P and Chausy J 1992 *Phys. Rev.* B **46** 922